Physiol. Res. 52: 481-496, 2003

Cauda Equina Syndrome and Nitric Oxide Synthase Immunoreactivity in the Spinal Cord of the Dog

J. MARŠALA, J. KAFKA[1], N. LUKÁČOVÁ, D. ČÍŽKOVÁ, M. MARŠALA[2], N. KATSUBE[3]

Institute of Neurobiology, Slovak Academy of Sciences, [1]Department of Neurosurgery, Medical Faculty, Šafárik University, Košice, Slovak Republic, [2]Anesthesiology Research Laboratory, University of California, San Diego, CA, U.S.A. and [3]Minase Research Institute, Ono Pharmaceutical Company, Ltd., Osaka, Japan

Received July 9, 2002
Accepted October 7, 2002

Summary

The development of the cauda equina syndrome in the dog and the involvement of spinal nitric oxide synthase immunoreactivity (NOS-IR) and catalytic nitric oxide synthase (cNOS) activity were studied in a pain model caused by multiple cauda equina constrictions. Increased NOS-IR was found two days post-constriction in neurons of the deep dorsal horn and in large, mostly bipolar neurons located in the internal basal nucleus of Cajal seen along the medial border of the dorsal horn. Concomitantly, NOS-IR was detected in small neurons close to the medioventral border of the ventral horn. High NOS-IR appeared in a dense sacral vascular body close to the Lissauer tract in S1-S3 segments. Somatic and fiber-like NOS-IR appeared at five days post-constriction in the Lissauer tract and in the lateral and medial collateral pathways arising from the Lissauer tract. Both pathways were accompanied by a dense punctate NOS immunopositive staining. Simultaneously, the internal basal nucleus of Cajal and neuropil of this nucleus exhibited high NOS-IR. A significant decrease in the number of small NOS immunoreactive somata was noted in laminae I-II of L6-S2 segments at five days post-constriction while, at the same time, the number of NOS immunoreactive neurons located in laminae VIII and IX was significantly increased. Moreover, high immunopositivity in the sacral vascular body persisted along with a highly expressed NOS-IR staining of vessels supplying the dorsal sacral gray commissure and dorsal horn in S1-S3 segments. cNOS activity, based on a radioassay of compartmentalized gray and white matter regions of lower lumbar segments and non-compartmentalized gray and white matter of S1-S3 segments, proved to be highly variable for both post-constriction periods.

Key words
Cauda equina syndrome • Nitric oxide synthase • Spinal cord • Dog

Introduction

Functional disorders that arise after cauda equina compression, classified clinically as cauda equina syndrome (CES), may be caused by herniated lumbar discs (De Palma and Rothman 1970, Crock and Yoshizawa 1976, Gathier 1976, Wiesel *et al.* 1984, Cricun and Cricun 1988, Gleave and MacFarlane 1990, Boden *et al.* 1990), compressing L3-S5 nerve roots in humans to a different extent and in varying intensities by means of spinal stenosis (Bartleson *et al.* 1983, Humphrey 1990, Haldeman and Rubinstein 1992) or by

Fax +420 241 062 164
E-mail: physres@biomed.cas.cz http://www.biomed.cas.cz/physiolres

compression caused by spinal neoplasmas (Gilbert *et al.* 1978) or metastatic tumors (Yap *et al.* 1978, Aroney *et al.* 1981, Tsukada *et al.* 1983, Sorensen *et al.* 1984, Hitchins *et al.* 1987, Jaradeh 1993). In the last decade, several canine (Delamarter *et al.* 1990, Konno *et al.* 1995a,b, Sato *et al.* 1995, Mao *et al.* 1998), porcine (Olmarker *et al.* 1989a,b, Pedowitz *et al.* 1989, Olmarker *et al.* 1990a,b,c, Olmarker 1991, Olmarker *et al.* 1991, Olmarker and Rydevik 1992, Olmarker *et al.* 1992, 1993, Rydevik 1993, Konno *et al.* 1995a, Cornefjord *et al.* 1996, 1997) and rat (Kawakami and Tamaki 1992, Iwamoto *et al.* 1995, Sayegh *et al.* 1997, Yamaguchi *et al.* 1999) models of compression-induced cauda equina syndrome have been used to assess the consequences of the compression of lower lumbar and sacral nerve roots on vascular and neural anatomy, cortical evoked potentials, impairment of impulse propagation and changes in neurotransmitters. In addition, correlative behavioral, neurological, neurophysiological and morphological analyses have been performed. However, recent efforts to assess and describe pathophysiological mechanisms have indicated that mechanical stimulation of the affected lumbosacral nerve roots results not only in anatomical and functional changes of affected nerve roots, but may also involve gray and white matter of the lumbosacral segments. In an attempt to identify the extent and intensity of the involvement of intrinsic spinal cord neurons following an acute or persistent cauda equina compression, a model of somatovisceral pain consisting in multiple cauda equina constrictions (MCEC) was used (Maršala *et al.* 1995). Surprisingly, a clearly expressed anterograde degeneration of sacrococcygeal and L7 dorsal root fibers was detected in S1-S3 and lower lumbar segments along with a narrow band of degenerated gracile fascicle. Moreover, a transneuronal degeneration of middle-sized and large neurons was noted in S1-S3 segments and, sporadically, in L7 segments. Concomitantly, a fully developed retrograde degeneration was reported affecting motoneurons in the ventrolateral portion of the ventral horn in S1-S3 segments (Maršala *et al.* 1995). A recent study, using the same model of incipient cauda equina syndrome in the dog, confirmed that segmental and laminar distribution of Fos-like immunoreactivity and nicotinamide adenine dinucleotide phosphate diaphorase (NADPH-d) positivity and double-labeled Fos-like immunoreactivity and NADPHd staining of neurons could be detected in lower lumbar and sacral segments of the canine spinal cord (Orendáčová *et al.* 2000, 2001). Both the above-mentioned studies have clearly demonstrated that the post-constriction response of intrinsic spinal neurons and, probably of ascending sensitive pathways is also prompt and may be related to the pain-processing microcircuits in the dorsal horn (Grzybicki *et al.* 1996), including NOS-containing and NO-synthesizing neurons, which might possibly play a role in the pathogenesis of the cauda equina syndrome. The aims of the present study were (i) to map and to compare the segmental and laminar distribution of NOS-IR neurons in the dog at different cauda equina post-constriction times in the lumbosacral segments, and (ii) to assess the possible changes of the catalytic NOS activity in compartmentalized gray matter regions and white matter columns of the lumbar and sacral segments.

Methods

Adult mongrel dogs (n=18) of both sexes (weighing 5-12 kg) were used in all the experiments. This experimental protocol was approved by the Institutional Animal Care and Use Committee of the Institute of Neurobiology, Slovak Academy of Sciences, Košice.

Experimental design and surgical procedures

The dogs were anesthetized with a mixture of ketamine and xylazine (100 mg/kg and 15 mg/kg b.w., i.m.) and artificially ventilated by a respirator with oxygen and nitrous oxide (Anemat N8 Chirana, CSSR). A lumbar laminectomy of the sixth and seventh laminae was carried out in order to gain access to the cauda equina (Maršala *et al.* 1995). Constrictions of the dural sac were produced by tying four loosely constrictive ligatures using chromic gut 2 mm apart resulting in multiple cauda equina constrictions (MCEC) consisting of protracted stimulation of the central processes of dorsal root ganglia cells of L7, S1-S3, Co1-Co5 and ventral roots of the same segments (Fig. 1). After surviving for two days (n=6) and five days (n=6), the animals were divided into two subgroups and processed separately for neuronal NOS (nNOS) immunocyto-chemistry after two days (n=3) and five days (n=3) post-constriction and for catalytic nNOS activity after two days (n=3) and five days (n=3) postconstriction. Sham-operated animals (n=6) underwent sham surgery (cauda equina exposure without ligation) and two days of postsurgery survival. Three animals of this group were used for nitric oxide synthase radioassay and three were processed for nNOS immunocytochemistry.

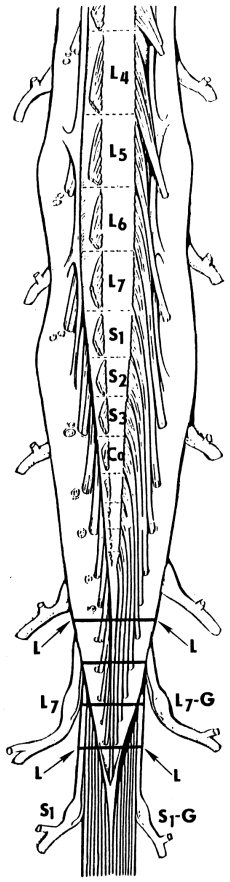

Fig. 1. *Schematic drawing depicting the position of four loosely tightened constrictions around cauda equina (L,L); L7-G and S1-G point to the corresponding dorsal root ganglia.*

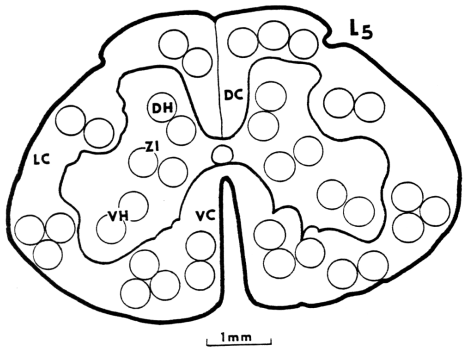

Fig. 2. *The specimens from 600 µm thick transverse sections of L4-L7 segments were punched by needles (id 0.6 or 0.8 mm) on a plate cooled in liquid nitrogen (–15 ºC). The punches were done separately from laminae I-VI (dorsal horns -DH), laminae VII and X (intermediate zone - IZ), laminae VIII-IX (ventral horns - VH), dorsal columns (DC), lateral columns (LC), ventral columns (VC). Punches (DH, IZ, VH, DC, LC, VC) were taken separately from spinal cord segments, pooled into a single sample and used for biochemical analysis.*

Sample dissection

Experimental animals used for radioassay detection of catalytic nitric oxide synthase (cNOS) activity were reanesthetized after survival and the access to the lumbar and sacral spinal cord was achieved by laminectomy. The spinal cord was then carefully dissected out and frozen in liquid nitrogen. The respective segments (L4-L7, S1-S3) and the cauda equina were cut by cryostat at –12 ºC in 600 µm slices. For a regional distribution of cNOS activity, spinal cord segments (L4-L7) were divided into the gray matter regions, i.e. dorsal horn (laminae I-VI), intermediate zone (laminae VII and X), ventral horn (laminae VIII-IX) and white matter regions, i.e. dorsal, lateral and ventral columns (Fig. 2). Spinal cord regions were punched under a surgical microscope by needles (id 0.4 and 0.6 mm) on a plate cooled with liquid nitrogen (–15 ºC). Sacral segments (S1-S3) were simply divided into white matter and gray matter.

Neuronal nitric oxide synthase immunocytochemistry

At the end of the survival periods, dogs were deeply anesthetized with sodium pentobarbital (50 mg/kg i.v.) and transcardially perfused with heparinized saline followed by perfusion with 4 % paraformaldehyde in a phosphate buffer (PB, pH 7.4). Four hours later, complete spinal cords were removed and were postfixed in the same fixative overnight at 4 ºC followed by immersion in sucrose (20 %) in phosphate buffered saline (PBS). Transverse cryostat sections (30 µm thick) were cut through lumbar (L), sacral (S) and coccygeal spinal cord segments, ten serial sections from each segment. Free floating sections were immediately processed for immunocytochemical staining (Bredt *et al.* 1990) with sheep antiserum against nNOS (Herbison *et al.* 1996) using the Vectastain ABC Elite kit (Vector Lab, Inc, Burlingame, USA).

Free floating sections from each spinal cord segment were placed in PBS, 0.1 M (pH=7.4) containing 5 % rabbit serum (RS), 0.2 % Triton X100 (TX) and 0.2 % bovine serum albumin (BSA) for 3 h at room temperature to block the non-specific protein activity. This was followed by one day incubation using a sheep nNOS antibody diluted 1:1500 in PBS containing 0.2 % TX-100 at 4 ˚C.

After treatment with the primary nNOS antibody, sections were washed several times in PBS and then incubated in biotinylated anti-sheep secondary antibody 1:200 for 2 h. The bound specific antibodies reacted with the avidine-biotin peroxidase solution for 1 h

and were visualized by using 0.05 % 3,3,4,4-diaminobenzidine hydrochloride (DAB) in 0.05 M Tris buffer containing 0.001 % H_2O_2. All sections were mounted on slides, dried, dehydrated and coverslipped with Permount. Negative controls were applied by omitting the primary antibody.

Nitric oxide synthase radioassay

The radioassay detection of cNOS activity was determined by the conversion of [^{3}H]-arginine to [^{3}H]-citrulline according to the method of Bredt and Snyder (1990) with a slight modification by Strosznajder and Chalimoniuk (1996). Frozen samples of the spinal cord were divided into two parts and separately homogenized in 100-150 µl of an ice-cold Tris-HCl buffer (10 mM, pH=7.4). Aliquots of homogenates (200 µg/ml), carried out in triplicate, were incubated for 45 min (37 ºC) with 10 µM [^{3}H] L-arginine (1 µCi), 1 mM NADPH, 1 µM calmodulin in a Hepes buffer (50 mM, pH=7.4) containing 1 mM dithiothreitol (DTT), 1 mM ethylene-diaminetetraacetic acid (EDTA), 100 µM flavin mononucleotide (FMN), 100 µM flavin adenine dinucleotide (FAD), 2 mM $CaCl_2$, 15 µM tetrahydro-biopterin (H_4B) in a final volume of 300 µl. The reaction was stopped by an addition of 1 ml of ice-cold Hepes buffer (100 mM, pH =5.5) containing 10 mM EDTA. Samples were applied to a Dowex AG 50W-X8 cationic-exchange column (Na^+ form) in order to remove the [^{3}H]-L-arginine. The columns were washed with 2 ml of deionized water to elute the [^{3}H]-L-citrulline. Samples were centrifuged at 1 000 x *g* for 5 min and aliquots (0.5 ml) of supernatant fractions were mixed with 5 ml of Bray's fluid into scintillation vials and then counted in a Beckman LS-3801 spectrometer. Cpms were converted to dpms using [^{3}H]-quenched standards. Levels of [^{3}H]-citrulline were computed after subtracting the blank which represented nonspecific radioactivity in the absence of enzyme activity. Protein determination was done according to Bradford (1976). The results were expressed as dpm/µg protein. The percentage distribution of cNOS activity was calculated from control values (taken as 100 %).

Laminar quantitative distribution of NOS-IR somata was counted from 10 serial sections of three animals (n=3) in the control group and three animals (n=3) surviving five days post-constriction. Profiles counting of all NOS-immunoreactive neurons occurring in the corresponding laminae was performed. Transverse sections were prepared from L6-S2 segments and the number of NOS-IR somata in the control group was compared with animals surviving five days post-constriction. The results were statistically evaluated by ANOVA as well as by the Tukey-Kramer test. The data are given as means ± S.E.M. $P<0.05$ value was considered significant when compared to the controls.

Statistical analysis

The results of nNOS immunoreactivity along with the radioassay detection of cNOS activity were statistically evaluated by ANOVA as well as by the Tukey-Kramer test and have been given as means ± S.E.M.

Results

Segmental and laminar distribution of nitric oxide synthase immunoreactivity in the lumbar and sacro-coccygeal spinal cord in sham- operated animals

In the transverse sections of lower lumbar and sacrococcygeal segments three components of NOS-IR staining could be detected. First, somatic NOS-IR involving spinal cord neurons of various types was found in the superficial (laminae I-II) and deep (laminae III-VI) dorsal horn layers along the rostrocaudal axis of all segments studied (Fig. 3A). However, considerable differences could be detected in the intensity of NOS-IR staining. While small NOS-IR neurons occurring in laminae I-II appear as lightly-stained round or elongated elements with poorly branched dendrites, the staining of many large multipolar NOS-IR neurons occurring in the deep dorsal layers was graded from light- to dark-brown. Similar NOS-IR neurons were present around the central canal in the lower lumbar segments close to the subependymal layer (lamina X) and along the lateral margin of the intermediate zone (lamina VII). The most pronounced somatic NOS-IR was found in the internal basal nucleus of Cajal located along the medial border of the dorsal horn in the lower lumbar and sacral segments (Fig. 3B). This contained large, mainly bipolar neurons with two thick long-stem dendrites, one reaching into the dorsal horn and another pointing to the dorsal commissure or even crossing to the opposite side and ending in the pericentral gray matter (Fig. 3E). An up-to-date, unidentified, irregularly shaped and rostrocaudally oriented cell column with a clearly expressed somatic NOS-IR was detected in the dorsomedial and central portion of the ventral horn and in the medial part of the intermediate zone in L4 to S2 segments corresponding to the lumbar enlargement (Figs 3C, 3D and 4). The majority of the medium-sized and large multipolar

NOS-IR neurons were located in laminae VII-IX. However, the neurons located in lamina VIII clearly prevailed over those located in the border zone around the gray matter of the ventral horn. Long dendrites of these neurons were often seen to penetrate into the white matter of the lateral and ventral columns or, occasionally, an axon-like process was seen to enter the lateral or ventral columns.

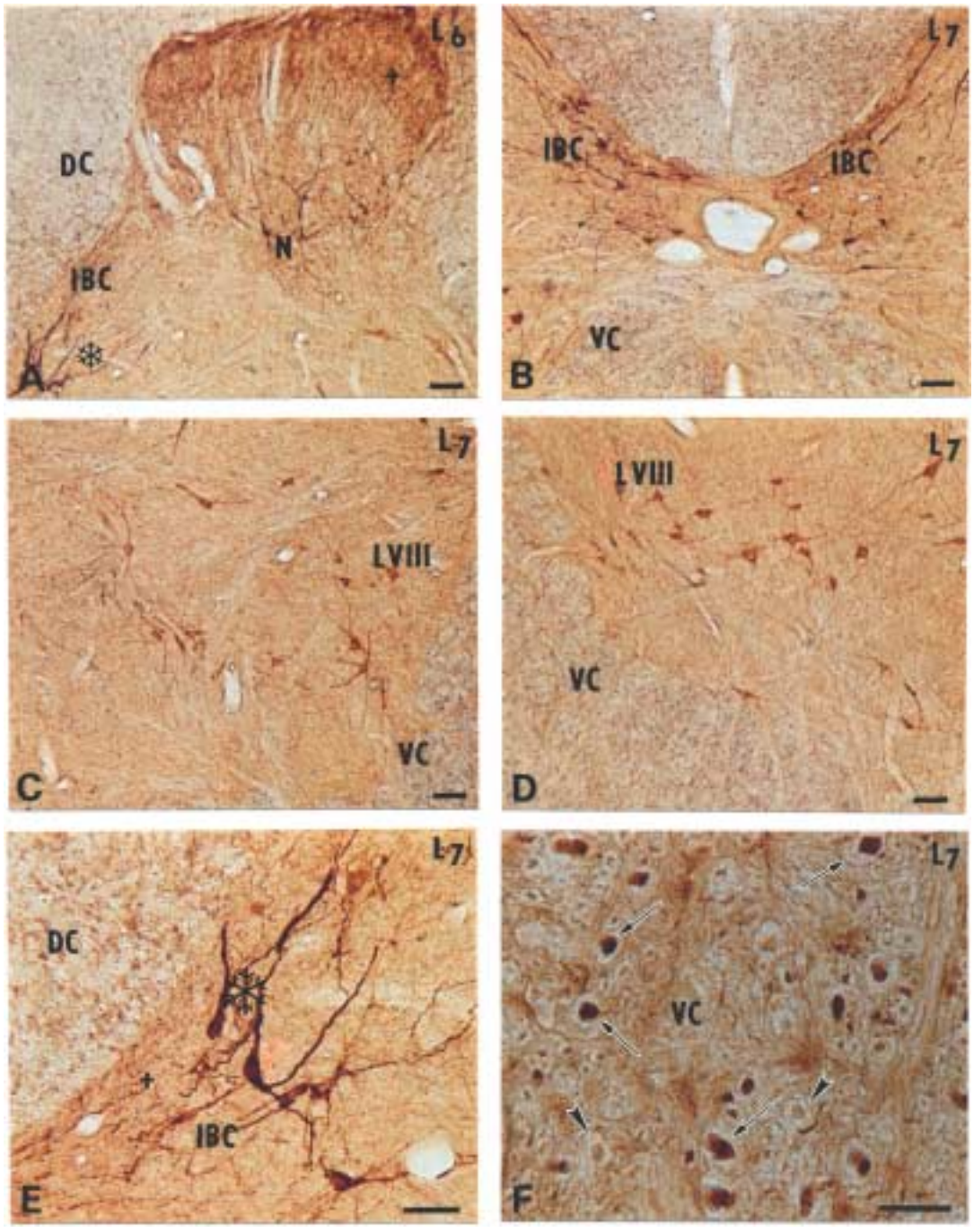

Fig. 3. *Microphotographs showing the distribution of somatic, fiber-like, punctate and axonal NOS immunopositivity in the L6 and L7 segments.* ***A,B*** *– somatic (N), fiber-like (asterisk) and punctate (cross) NOS immunopositivity are seen in the dorsal horn and internal basal nucleus of Cajal (IBC); DC, dorsal column; VC, ventral column.* ***C,D*** *– the distribution of NOS-IR somata in the dorsomedial region of the ventral horn (LVIII); VC, ventral column.* ***E*** *– somatic (asterisk), fiber-like and punctate (cross) NOS immunopositivity in the internal basal nucleus of Cajal (IBC); DC, dorsal column.* ***F*** *– thick NOS immunopositive (arrows) and NOS immunonegative axons (arrowheads) in the ventral column (VC). Bars A,B,C,D and F = 100 μm; E = 50 μm.*

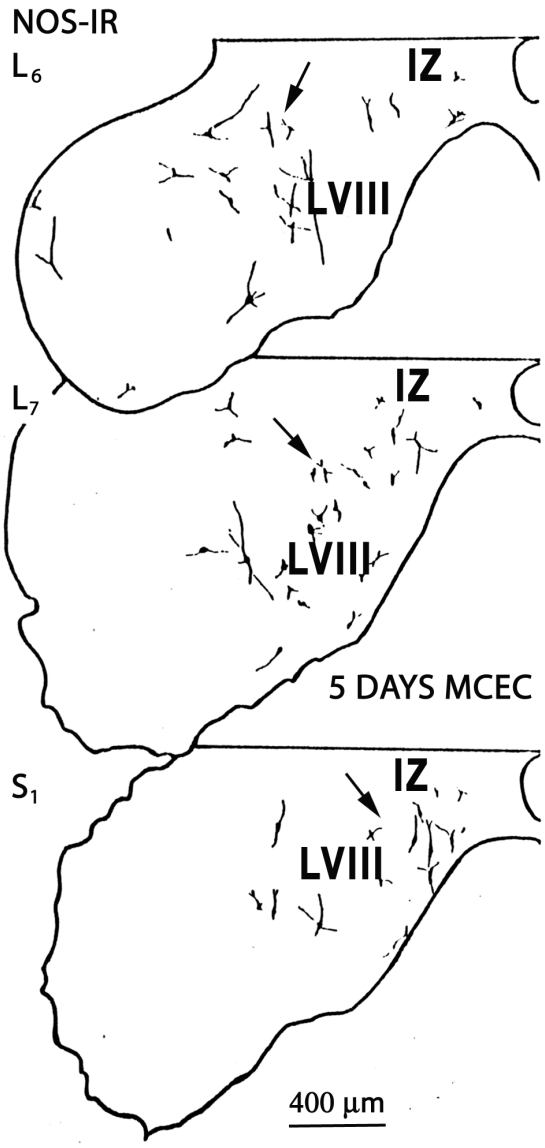

Fig. 4. *Camera lucida drawing depicting the location of NOS immunopositive somata (arrows) in the dorsomedial portion of the ventral horn (LVIII) and intermediate zone (IZ). Transverse sections cut through the upper portion of L6-S2 segments.*

The patterns of the fiber-like NOS-IR may be arbitrarily divided into two groups for analyzing the occurrence of NOS-IR fibers in the gray or white matter of the lower lumbar and sacral segments. Short fiber-like fragments that are rarely covered by spines are currently seen in the superficial dorsal horn (laminae I-II). They may be a part of the dendritic branches of small NOS-IR somata identified in the same layers or may come from terminal ramifications of the thin unmyelinated axons (C-fibers) entering the dorsal horn *via* the dorsal roots. Similar NOS-IR fragments could be seen in the neuropil around the central canal (lamina X) and in the dorsal gray commissure. However, the existence of short NOS-IR fragments at both sites is often obscured by densely packed NOS-IR puncta. A quite different pattern of fiber-like NOS immunoreactivity was found in the deep dorsal horn layers (laminae III-VI) along the rostrocaudal axis. This consisted of thick, often tortuous and spinous dorsoventrally oriented fibers sometimes traceable to the pericentral region. The course and the ramification pattern suggest that they are dendrites of the large multipolar NOS-IR somata described in laminae III-VI. A highly differentiated fiber-like NOS-IR pattern of large bipolar neurons occurring in the internal basal nucleus of Cajal was seen along the medial border of the dorsal horn of all lumbosacral segments. Dendritic ramifications were arranged in such a way that dorsally oriented thick stem dendrites were running in the dorsal direction traceable into the medial dorsal horn, while dendrites oriented in an opposite direction were oriented ventromedially into the dorsal commissure (Figs 3B and E).

Punctate, non-somatic NOS staining found in the neuropil of some gray matter regions formed the third component of NOS immunoreactivity in the lumbosacral segments. Superficial dorsal horn (laminae I-II) in all segments studied, dorsal gray commissure (DGC) in S1-S3 segments and the Onuf's nucleus in S1-S3 segments proved to be sites of high punctate NOS-IR. In the superficial dorsal horn and DGC the density and staining of NOS-IR puncta were found to be almost homogeneously distributed across the mediolateral extent of the superficial dorsal horn and DGC. In contrast, the punctate NOS-IR in the neuropil of the Onuf's nucleus appeared as a dense accumulation of NOS-IR puncta around NOS-immunoreactive neurons of Onuf's nucleus. High power magnification revealed that the majority of NOS-IR puncta at all these loci range between 0.5-0.7 µm in diameter.

Surprisingly, a high number of axonal NOS-IR profiles was detected in the white matter of lower lumbar and sacral segments. Numerous, mostly thin NOS-IR axons were found in the dorsolateral funiculus in all segments and in the juxtagriseal portion of the lateral column of the lumbar enlargement. A massive occurrence of NOS-IR axonal profiles was detected in the juxtagriseal layer of the ventral column all along the lumbosacral segments. Prominent, non-varicose, large-caliber NOS-IR axons were present throughout the rostrocaudal extent in the ventrolateral portion of the

lateral and ventral columns, being most prevalent in the medial portion of the ventral column (Fig. 3F). Finally, at lower lumbar and sacral levels, a clearly expressed axonal NOS-IR was found in the Lissauer tract and along the lateral and medial border of the dorsal horn corresponding with the location of the lateral (LCP) and medial (MCP) collateral pathways, respectively.

Table 1. The number of NOS-IR neurons in laminae I-II, laminae III-VI, laminae VII and X and laminae VIII-IX in lower lumbar (L6, L7) and sacral (S1, S2) segments of the dog spinal cord in control and five days after multiple cauda equina constrictions (MCEC).

Segment	Experimental groups	Laminae			
		I-II	III-VI	VII and X	VIII and IX
L6	Control	22.86±0.78	13.07±0.64	10.87±0.43	21.93±0.23
	MCEC (5 days)	6.90±0.50*	12.83±0.76	11.13±0.73	28.66±1.51*
L7	Control	20.77±0.57	12.37±0.75	11.43±0.38	20.13±0.84
	MCEC (5 days)	7.83±0.166*	12.76±0.87	12.30±0.66	25.23±0.68*
S1	Control	18.03±0.38	11.60±0.45	11.76±0.20	19.90±0.71
	MCEC (5 days)	7.66±0.18*	12.76±0.97	12.83±0.98	27.00±0.42*
S2	Control	18.46±0.38	13.90±0.25	10.93±0.58	21.03±0.41
	MCEC (5 days)	10.73±0.23*	12.46±0.35*	14.90±0.23*	26.60±0.27*

**p<0.05 with respect to the controls*

Segmental and laminar patterns of nitric oxide synthase immunoreactivity in lumbar and sacral segments two and five days after MCEC

Two days after MCEC, two sets of NOS-IR neurons appeared to respond quite promptly to the constriction of the central processes of the primary afferent neurons forming a part of the cauda equina. An enhanced NOS-IR was noted in the superficial and deep dorsal horn and in large bipolar NOS-IR neurons located in the internal basal nucleus of Cajal along the medial border of the dorsal horn, with intensely NOS immunopositive thick and long dendrites extending in the dorsal and ventral direction (Figs 5A, 5B and 5C). Concomitantly, NOS-IR appeared in a few small neurons at the medioventral border of the ventral horn in lumbar and sacral segments (LS). The contours of the soma were seen to have a diameter of 10-15 μm and proximal dendrites, extending to a radius of about 100-150 μm, some going out in the ventral white column (Fig. 5D). Unusually high NOS-IR was found laterally to the dorsal horn and along the ventral border of the Lissauer tract in a location where a dense vascular plexus could be seen (Fig. 5E) and in DGC containing reach the NOS-IR capillary network and NOS-IR arterioles (Fig. 5F).

Prominent changes in somatic and fiber-like NOS-IR were noted five days after MCEC. High NOS-IR in the Lissauer tract, seen in all LS segments studied, was accompanied by a clearly expressed fiber-like and punctate, non-somatic NOS-IR seen not only in the superficial dorsal horn but also in the lateral (LCP) and medial (MCP) collateral pathways (Figs 6A and 6B). Thin bundles of NOS-IR fibers of MCP were found intermingled with NOS-IR large bipolar neurons in the internal basal nucleus of Cajal as noted before (Fig. 6C). A quantitative assessment of somatic NOS-IR performed in different laminae of L6-S2 segments revealed a highly controversial lamina-dependent response of NOS-IR somata. The number of small NOS-IR somata that were easily identified in control sections of laminae I-II was significantly decreased in the extent of the lumbar enlargement, while the number of large NOS-IR somata occurring in laminae III-VI, with the exception of S2 segment, was not significantly changed (Table 1). Contrary to the previous finding, the number of middle-sized and large NOS-IR somata located in laminae VIII and IX was significantly increased and, moreover, many NOS-IR neurons in laminae VIII and IX exhibited intense dendritic NOS immunopositivity (Fig. 6D,E). Finally, in the intermediate zone (lamina VII) and pericentral region (lamina X) a significant increase of NOS-IR somata was found only in the S2 segment. A high NOS-IR of the sacral vascular body and vessels supplying DGC could be seen at five days post-constriction (Fig. 6F).

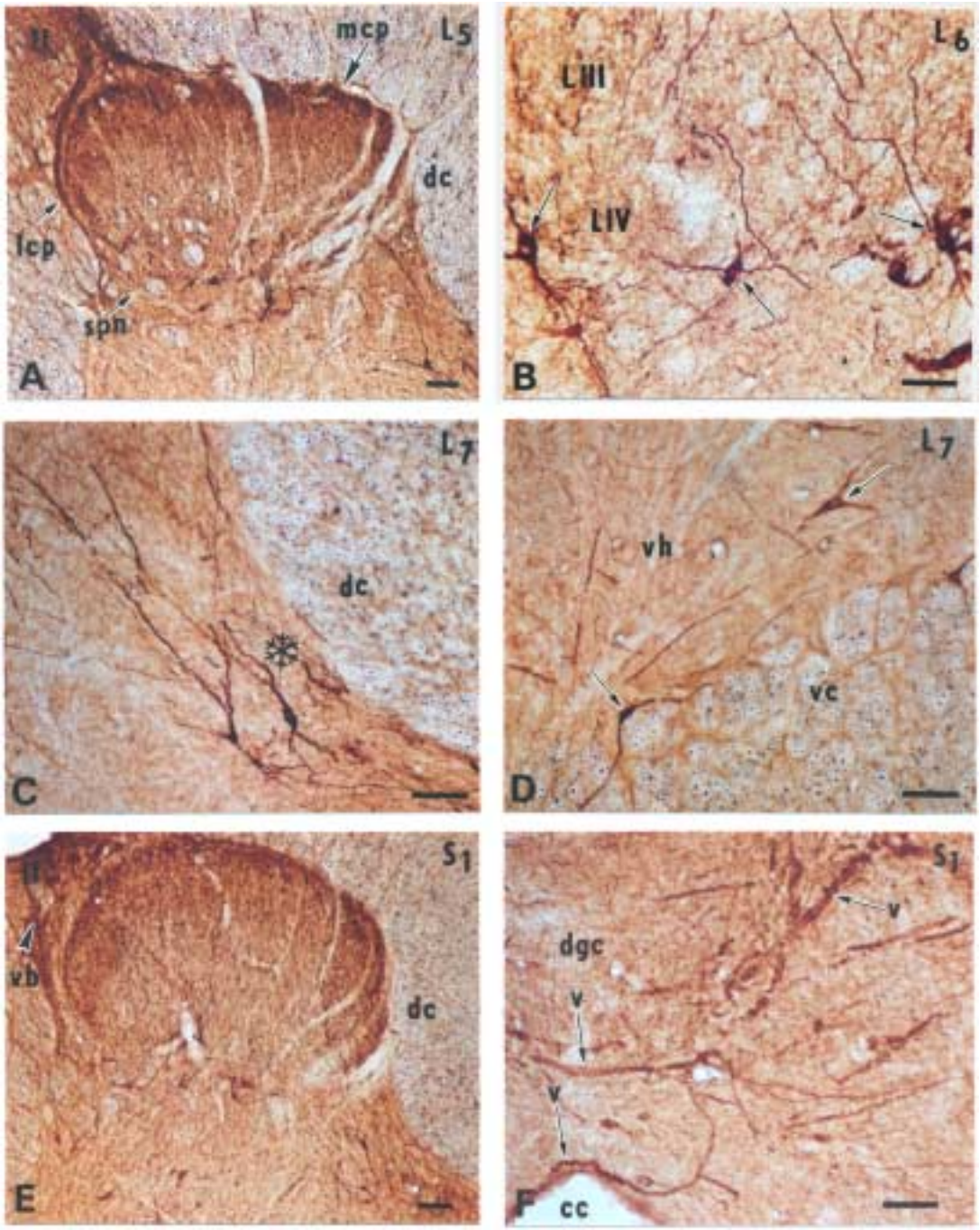

Fig. 5. *Microphotographs showing the response and distribution of NOS-IR in L4-S1 segments two days after cauda equina constrictions.* ***A*** *– superficial and deep dorsal horn; dc - dorsal column; lt - Lissauer tract; lcp - lateral collateral pathway; spn - sacral parasympathetic nucleus; arrow points to NOS-IR fibers running along the outer border of the dorsal horn and forming the medial collateral pathway (mcp).* ***B*** *– high somatic (arrows) NOS immunopositivity in the deep dorsal horn layers (LIII-LIV).* ***C*** *– clearly expressed NOS-IR in the internal basal nucleus of Cajal (asterisk); dc - dorsal column.* ***D*** *– the appearance of small highly NOS immunoreactive neurons (arrows) along the ventrolateral periphery of the ventral horn (vh); vc - ventral column.* ***E*** *– intensely stained NOS-IR vascular body (vb) just below the Lissauer tract (lt) and laterally to the dorsal horn; dc - dorsal column.* ***F*** *– high NOS immunopositivity (arrows) of vessels (v) supplying the dorsal gray commissure (dgc); cc - central canal. Bars A,E and F = 100 μm; B,C and D = 50 μm.*

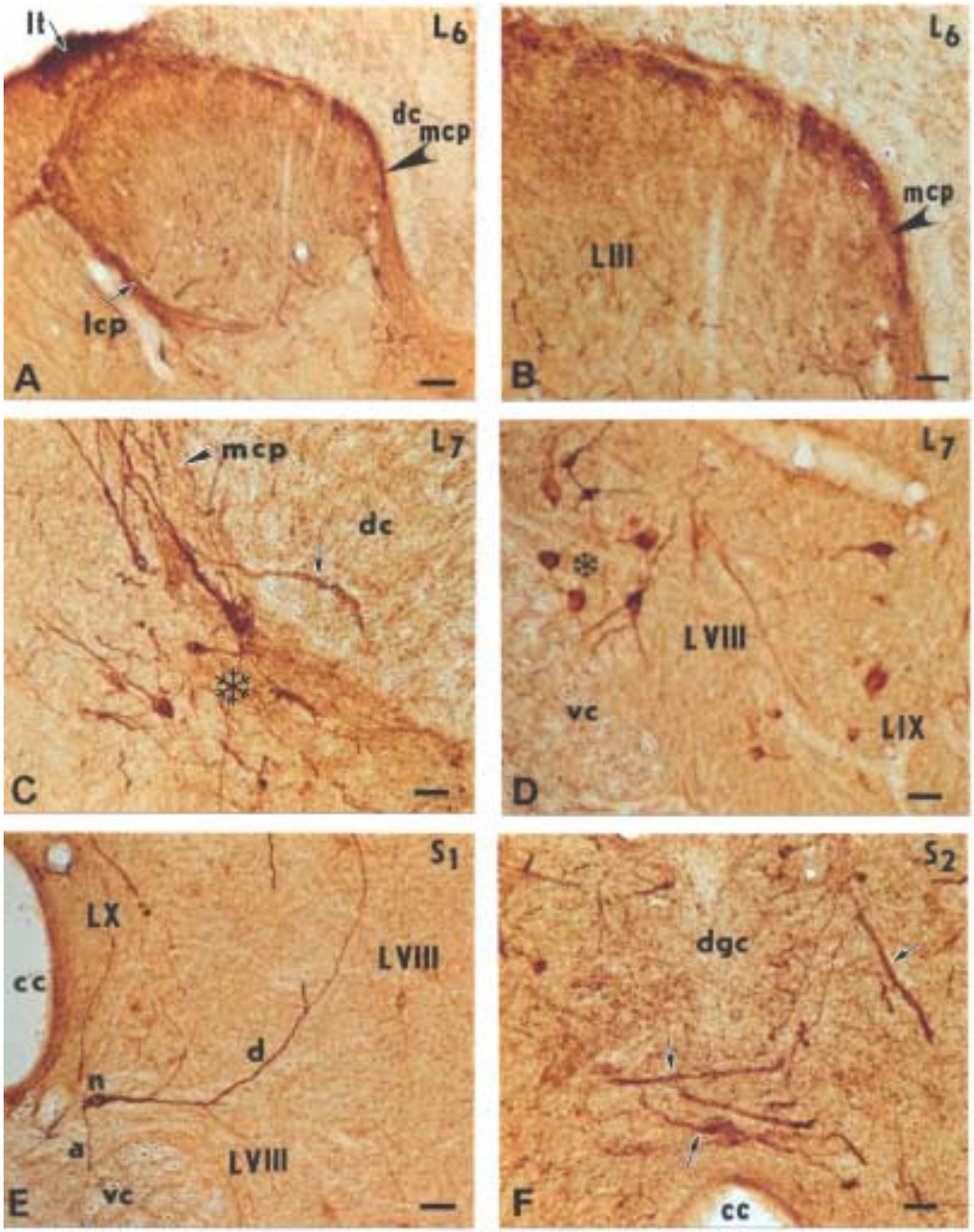

Fig. 6. *Microphotographs showing the distribution of NOS-IR in L6-S2 segments five days after cauda equina constrictions.* ***A*** *– superficial and deep dorsal horn; dc - dorsal column; lt - Lissauer tract; lcp - lateral collateral pathway; arrow points to a dense accumulation of punctate NOS-IR in the medial dorsal horn and medial collateral pathway (mcp).* ***B*** *– medial dorsal horn showing high NOS immunopositivity (arrow).* ***C*** *– the internal basal nucleus of Cajal (asterisk) and medial collateral pathway (mcp); dc - dorsal column; arrow points to NOS-IR vessel in the dorsal column.* ***D*** *– a highly NOS immunopositive group of neurons (asterisk) in the dorsomedial portion of the ventral horn (LVIII-LIX); vc - ventral column.* ***E*** *– large NOS-IR neurons in the pericentral region (lamina X) with a dendrite ramifying in laminae LVII-LVIII (d) and axon (a) entering the dorsal portion of the ventral column (vc); cc - central canal.* ***F*** *– high NOS immunopositivity of vessels (arrows) in the ventral portion of the sacral dorsal gray commissure (dgc). Bars A = 100 μm; bars B,C,D,E and F = 50 μm.*

Table 2. Percentage distribution of catalytic nitric oxide synthase (cNOS) activity in gray matter and white matter in cauda equina and in sacral segments (S1-S3), two and five days after multiple cauda equina constrictions (MCEC).

Spinal cord regions	dpm/μg protein	
	2 days after MCEC	5 days after MCEC
Gray matter	55.6±1.7*	127.6±2.2*
White matter	45.0±1.7*	130.8±8.5
Cauda equina	34.1±2.7*	72.9±1.8*

*The enzyme activity was determined by the conversion of [^{3}H]-arginine to [^{3}H]-citrulline (dpm/μg protein). The results were expressed as percentage of control values. Data are given as means ± S.E.M. of nine separate experiments (carried out in triplicate) *P<0.05 with respect to controls.*

The distribution of catalytic nitric oxide synthase activity in the gray matter regions and white matter columns in the lumbosacral segments and cauda equina two and five days after MCEC

The radioassay of cNOS activity was performed in region-specified samples of the gray and white matter of lumbar (L4-L7) and sacral (S1-S3) segments, including samples of the cauda equina. Significant changes of cNOS activity were noted at both post-constriction periods in the cauda equina comprising the nerve roots of lumbar (L7) and sacral (S1-S3) segments. Non-compartmentalized gray matter of S1-S3 segments proved to be highly versatile since, at two post-constriction days, a significant decrease followed by a significant increase of cNOS could be detected at five days while, in the non-compartmentalized white matter, a significant decrease of cNOS activity was apparent only at two days post-surgery (Table 2). A more complex response of NO-synthesizing neurons appeared in the compartmentalized gray and white matter in the L4-L7 segments two and five days post-constriction. While a significant decrease of cNOS activity was found in the dorsal horn (laminae I-VI) at two days post-surgery, followed by a mild decrease at five days, cNOS activity in the intermediate zone (lamina VII) and pericentral region (lamina X) was comparable with that seen in control samples. In the ventral horn (laminae VIII and IX) a significant increase of cNOS activity was found five days post-constriction. With regard to the white matter, all three columns exhibited a significant increase of cNOS activity at two days postoperatively (Table 3).

Table 3. Percentage distribution of catalytic nitric oxide synthase (cNOS) activity in gray matter regions, i.e. dorsal horn (laminae I-VI), intermediate zone (laminae VII and X), ventral horn (laminae VIII-IX) and white matter columns (dorsal, lateral and ventral) in lower lumbar segments (L4-L7), two and five days after multiple cauda equina constrictions (MCEC).

Spinal cord regions	dpm/μg protein	
	2 days after MCEC	5 days after MCEC
Dorsal horn	78.0±2.0*	85.6±2.4
Intermediate zone	98.2±1.7	113.6±3.8
Ventral horn	101.0±1.4	175.3±7.7*
Dorsal column	174.9±9.0*	114.1±4.8
Lateral column	229.9±3.8*	109.4±6.5
Ventral column	237.9±2.4*	113.3±6.2

*The enzyme activity was determined by the conversion of [^{3}H]-arginine to [^{3}H]-citrulline (dpm/μg protein). The results were expressed as percentage of control values. Data are given as means ± S.E.M. of nine separate experiments (carried out in triplicate) *P<0.05 with respect to controls.*

Neurological function were tested in all the animals before surgery and then daily for five days. Sudden motor and sensory disturbances of the lower limbs combined with acute bladder dysfunction were noted in both groups of animals subjected to multiple cauda equina constriction. While paraparesis was the most common finding in animals surviving two day postconstriction, during prolonged compression period, i.e. after five days a fully developed paraplegia appeared in all animals with MCEC.

Discussion

Single or two-level compression of the lower lumbar and sacral nerve roots by herniated lumbosacral discs, spinal stenosis, spinal neoplasmas, ischemic insults, arteriovenous malformations or fragments of the fractured bones may lead to the development of

a complex clinical entity called cauda equina syndrome (Aho *et al.* 1969, Jaradeh 1993). The occurrence of a polyradicular symptomatology and accompanying disorders such as low-back pain, saddle anesthesia, bladder and colon dysfunction, motor weakness of the lower extremities or chronic paraplegia suggests that several neuronal pools may be involved. These include cutaneous, muscular and visceral nociceptive sensitivity located in the lumbar and sacral segments. To date we have a very incomplete understanding of the neuropathogenesis of the sensitive disorders that occur when the nerve roots of the cauda equina are compressed or damaged. Polyradicular symptomatology and the heterogeneous nature of the sensitive disorders seen in the cauda equina syndrome suggest that sustained stimulation of afferent fibers carrying different sensitive modalities may play a significant role. The involvement of visceral primary afferent fibers from the pelvic (Morgan *et al.* 1981) and pudendal (Thor *et al.* 1989) nerves containing various types of afferent and efferent axons (Kuru 1965, Martin *et al.* 1974) may be of primary importance. The afferent axons of the pudendal nerve convey input to the sacral spinal cord from cutaneous receptors in the genitalia and perineal skin, tension receptors in the urethral and rectal striated musculature, and mucosal receptors in the urethra and anal canal (Barrington 1931, Bors 1952, Kuru 1965, Martin *et al.* 1974). The efferent fibers of this nerve, which are simultaneously constricted along with the afferent components, are composed of motor axons which originate in Onuf's nucleus in the sacral segments and sympathetic postganglionic axons that originate from neurons in the lower lumbar sympathetic chain ganglia (Kuo *et al.* 1984), which are not directly involved in MCEC. Multisegmental termination sites of afferents and the polyradicular origin of efferents both became constricted and stimulated in our experimental paradigm. This points to some differences between MCEC model in the dog and several neuropathic models, particularly if we also consider that the central and not the peripheral processes of the dorsal root ganglia neurons are constricted (Bennett and Xie 1988, Kim and Chung 1992, Steel *et al.* 1994, Choi *et al.* 1996, Shi *et al.* 1998, Ossipov *et al.* 1999). Since several lines of evidence have indicated a role of NO in nociceptive processing (Meller and Gebhart 1993), the expression and activity of NOS in the DRG neurons and spinal cord were studied in order to clarify the activation of nociceptive afferents, i.e. how this activation results in an increased excitability of spinal neurons in the pathogenesis of nerve injury-induced thermal hyperalgesia, mechanical allodynia and chronic neuropathic pain and in the development of a phenomenon known as central sensitization (Woolf 1983, Dubner and Ruda 1992, Coderre *et al.* 1993).

Previous studies have shown that an intrathecal injection of NMDA induces short-lasting hyperalgesia in mice and the application of an inhibitor of nitric oxide synthase, L-NAME, administered either systemically or intrathecally, blocked the NMDA-induced hyperalgesia (Kitto *et al.* 1992). Similarly, the intrathecal administration of L-arginine, but not of D-arginine, produced rapid, transient, dose-dependent facilitation of the nociceptive tail-flick reflex which was completely suppressed by prior treatment with either L-NAME or AP5 (Meller *et al.* 1992). These results suggest that NMDA-produced facilitation of a thermal nociceptive reflex mediated by activation of an NMDA receptor that results in an increase of endogenous NO and the activation of soluble guanylate cyclase in the lumbar spinal cord. Similarly, a recent study concerning NOS-IR in the lumbar dorsal root ganglia and spinal cord in rats and monkeys after peripheral axotomy disclosed that, after unilateral sciatic nerve section in the rat, the number of NOS-immunopositive neurons increased in the ipsilateral L4 and L5 dorsal root ganglias (DRGs) while NOS-IR was observed in the ipsilateral dorsal roots and in an increased number of NOS-IR fibers and terminals in both outer and inner lamina II of the ipsilateral dorsal horn. However, the number of NOS-IR somata in lamina II of the ipsilateral dorsal horn was reduced. Therefore, it was suggested that axotomy in rat induces a marked upregulation of NOS synthesis in primary sensory neurons. In the monkey, many small NOS-IR somata in L4 and L5 DRGs appeared but only a few weakly stained nerve fibers and terminals were found in laminae I-IV at L4 and L5 lumbar levels. Concurrently, a few NOS-IR somata were present in lamina X (Zhang *et al.* 1993). In a model of peripheral neuropathy induced by ligation of the left L5 and L6 nerve roots, a bilateral decrease in NOS activity, assayed separately from the right and left sides, was found in the lumbar spinal cord, while NOS activity was increased in the ipsilateral L5 and L6 DRGs following neuropathic surgery (Choi *et al.* 1996). Both observations are consistent with a previous finding reporting an ipsilateral increase in NOS-IR somata in the L5 and L6 DGRs in the same model (Steel *et al.* 1994). Nevertheless, the question why spinal NOS activity is bilaterally decreased still remains unanswered. This phenomenon seemingly contradicts the role that NO is supposed to play in nociceptive processes. The results of

the immunohistochemical NOS-IR analysis along with catalytic NOS activity performed during the incipient phase of the cauda equina syndrome in the dog results in an intense involvement of the NO synthesizing neuronal pools in the lumbosacral segments.

When regional and laminar patterns of somatic, fiber-like and punctate NOS immunoreactivity and cNOS activity, ensuing after MCEC in LS segments two and five days post-constriction, are compared with neuropathic pain models in the rat, considerable differences could be detected. Prominent NOS-IR was found in the Lissauer tract at the L6-S3 level, mainly five days post-constriction, and finely granulated NOS immunopositivity was seen to continue along the surface of the dorsal horn, forming narrow bundles traceable in two directions. A ventrolaterally oriented, intensely stained NOS-IR bundle seems to correspond with the location of the lateral collateral pathway (LCP), strongest in the region of S1-S3 segments and extending along the lateral dorsal horn into the lateral portion of laminae V and VI and terminating mostly in the gray matter of the sacral parasympathetic nucleus (SPN). The location of the lateral collateral NOS-IR pathway is consistent with the distribution of visceral primary afferents from the pelvic nerve to the Lissauer tract and the spinal gray matter identified by horse-radish peroxidase applied to the cut pelvic nerve (Morgan *et al.* 1981). A medially oriented NOS-IR bundle, classified as a medial collateral pathway (MCP – Morgan *et al.* 1981) and seen more clearly following longer post-constriction time, is in a close touch with lamina I and tends to move ventrally along the medial border of the dorsal horn, thus reaching the internal basal nucleus of Cajal. Occasionally, some NOS-IR fibers were seen to penetrate into the dorsal gray commissure (DGC). An increased punctate, non-somatic NOS-IR seen in the neuropil of the internal basal nucleus of Cajal, in DGC and in the medial third of the nucleus proprius and substantia gelatinosa, suggests that the fiber-like NOS-IR of the MCP may have a direct relationship with the afferent pathway of the pudendal nerve. This nerve is known to carry afferents from cutaneous receptors in the genitalia, perineal skin, tension receptors in the urethral and rectal striated musculature as well as from mucosal receptors in the urethra and anal canal (Bors 1952, Kuru 1965, Martin *et al.* 1974, Thor *et al.* 1989). It should be noted that a clearly expressed NOS-IR of the MCP is accompanied by a strongly enhanced NOS-IR of bipolar somata in the internal basal nucleus of Cajal.

A remarkable finding concerns the description of an unknown NOS-IR positive neuronal pool located in laminae VIII-IX in the region of the lumbar intumescence and containing small, medium-sized and large NOS-IR somata. While NOS-IR somata, easily recognized in control sections, were located mostly in the dorsomedial portion of the ventral horn, many NOS-IR neurons of the same type were dispersed across the mediolateral extent of the ventral horn, including the core region, occupied by lamina VII neurons, or along the ventromedial periphery of the ventral horn. Moreover, in the model of MCEC at five days post-constriction, many somata and dendrites expressed high NOS immunopositivity. It should be noted that no direct connection between NOS-IR somata in laminae VIII-IX and ventral roots could be detected. Moreover, no such NOS-IR somata were visible in the Onuf's nucleus and, quite rarely, NOS-IR could only be found in the neurons of the ventrolateral nucleus. It is known that both these nuclei respond to a unilateral transection and ligation of the pudendal nerve by a clear increase of somatic NOS-IR measured by micro-densitometry (Pullen and Humphreys 1999). It is noteworthy to mention that the occurrence of NOS immunoreactive neurons in the ventral horn have not yet been recognized, and only a few lightly stained neurons in the ventral horn have occasionally been observed. However, cellular staining within the ventral horn and ventral white matter was generally absent (Vizzard *et al.* 1994, 1997). At the lower lumbar and sacral levels in both control and MCEC dogs, a clearly definable column of NOS-IR neurons occurs in lamina VIII and, to a lesser extent, in lamina IX. This confirms that a NO-synthesizing pool in the lumbar enlargement, located in the dorsomedial portion of the ventral horn (lamina VIII), but not participating in the formation of the ventral root fibers, does really exist. More significantly, in the incipient phase of the cauda equina syndrome, these neurons are among the first which respond to MCEC by means of a strongly enhanced NOS immunopositivity. It should be mentioned that, regarding the laminar position and neuronal types, many of the above characterized neurons may belong to the category of long ascending propriospinal neurons that have been identified in the same spinal cord regions by retrograde and tract tracing studies (Barilari and Kuypers 1969, Matsushita *et al.* 1979). Concurrently, this finding significantly broadens the scope of spinal NOS-containing neurons and the putative role they may play therein (Blot *et al.* 1994, Yezierski *et al.* 1996).

An unexpectedly high NOS immunopositivity was found at two and five days postconstriction along the ventrolateral border of the Lissauer tract and the lateral border of the dorsal horn in S1-S3 segments. Large, irregularly shaped patches of NOS-IR continued ventrally and were traceable to the neck region of the dorsal horn. They appeared as a punctate, non-somatic NOS immunostaining often located in close association with small vessels which were occasionally seen to pass medially and to penetrate into the DGC. Here, a clear NOS immunopositive capillary network and larger arteriolar branches could be detected, mainly in the ventral third of the DGC. While the origin of the capillary and arteriolar NOS immunopositivity could not be revealed, two possible sources might be suspected to enhance the vessel NOS immunopositivity in this region. One may come from the lateral extension of the highly NOS immunopositive lateral portion of the Lissauer tract which blends in this region without a discrete border with the dorsolateral funiculus (Morgan *et al* 1981). Alternatively, the sustained stimulation of cauda equina afferents in this experimental paradigm might induce the expression of nitric oxide synthase type II in some resident cells, e.g. microglia, in the dorsal horn and Lissauer tract or, directly, in the endothelia of vessels supplying the dorsal horn and DGC similarly to conditions producing thermal hyperalgesia (Grzybicki *et al.* 1996).

Considering the fact that NO is a highly diffusible molecule, it can be hypothesized that in the MCEC model, neuronal activity in the sacral DGC could be affected not only by NO released from large NOS-IR neurons located in the DGC itself, but also by NO released *via* the activity of microglial and endothelial cells. The impact of this locally enhanced NOS activity in the DGC on direct connections coming from the pontine micturition center and influencing both the bladder detrusor muscle motoneurons and GABAergic inhibitory interneurons in the DGC (Blok *et al.* 1998) is as yet unknown.

Acknowledgements

The authors thank Mr. D. Krokavec, Ms. M. Špontáková, Mrs. M. Istvanová, Mrs. M. Vargová and Mrs. I. Vrábelová for their excellent technical assistance. The experimental work was supported by the VEGA Grants No. 2/7222/20, 2/1064/21 and 2/2079/22 from the SAS and by NIH grants NS 32794 and NS 40386 to M.M.

References

AHO AJ, AURANEN A, PERSONEN K: Analysis of cauda equina symptoms in patients with lumbar disc prolapse. *Acta Chir Scand* **135:** 413-420, 1969.

ARONEY RS, DALLEY DN, CHAN WK, BELL DR, LEVI JA: Meningeal carcinomatosis in small cell carcinoma of the lung. *Am J Med* **71:** 26-32, 1981.

BARILARI MG, KUYPERS HGJM: Propriospinal fibers interconnecting the spinal enlargements in the cat. *Brain Res* **14:** 321-330, 1969.

BARRINGTON FJF: The component reflexes of micturition in the cat. Parts I and II. *Brain* **54:** 177-188, 1931.

BARTLESON JD, COHEN MD, HARRINGTON TM, GOLDSTEIN NP, GINSBURG WW: Cauda equina syndrome secondary to long-standing ankylosing spondylitis. *Ann Neurol* **14:** 662-669, 1983.

BENNETT GJ, XIE YK: A peripheral mononeuropathy in rat that produces disorders of pain sensation like those seen in man. *Pain* **33:** 87-107, 1988.

BLOK BFM, VAN MAARSEVEEN JTPW, HOLSTEGE G: Electrical stimulation of the sacral dorsal gray commissure evokes relaxation of the external urethral sphincter in the cat. *Neurosci Lett* **249:** 68-70, 1998.

BLOT S, ARNAL JF, XU Y, GRAY F, MICHEL JB: Spinal cord infarcts during long-term inhibition of nitric oxide synthase in rats. *Stroke* **25:** 1666-1673, 1994.

BODEN SD, DAVIS DO, DINA TS, PATRONAS NJ, WIESEL SW: Abnormal magnetic resonance scans of the lumbar spine in asymptomatic subjects. *J Bone Joint Surg* **72-A:** 403-408, 1990.

BORS E: Effect of electrical stimulation of the pudendal nerves on the vesical neck; its significance for the function of cord bladders: a preliminary report. *J Urol* **67:** 925-935, 1952.

BRADFORD MM: A rapid and sensitive method for the quantitation of microgram quantities of protein utilizing the principle of protein-dye binding. *Anal Biochem* **72:** 248-254, 1976.

BREDT DS, SNYDER SH: Isolation of nitric oxide synthetase, a calmodulin-requiring enzyme. *Proc Natl Acad Sci USA* **87:** 682-685, 1990.

BREDT DS, HWANG PM, SNYDER SH: Localization of nitric oxide synthase indicating a neuronal role for nitric oxide. *Nature* **347:** 768-770, 1990.

CHOI Y, RAJA SN, MOORE LC, TOBIN JR: Neuropathic pain in rats is associated with altered nitric oxide synthase activity in neural tissue. *J Neurol Sci* **138:** 14-20, 1996.

CODERRE TJ, FUNDYTAS ME, MCKENNA JE, DALAL S, MELZACK R: The formation test: a validation of the weighed-scores method of behavioral pain rating. *Pain* **54:** 43-50, 1993.

CORNEFJORD M, OLMARKER K, RYDEVIK B, NORDBORG C: Mechanical and biochemical injury of spinal nerve roots: a morphological and neurophysiological study. *Eur Spine J* **5:** 187-192, 1996.

CORNEFJORD M, SATO K, OLMARKER K, RYDEVIK B, NORDBORG C: A model for chronic nerve root compression studies. Presentation of a porcine model for controlled, slow-onset compression with analyses of anatomic aspects, compression onset rate, and morphologic and neurophysiologic effects. *Spine* **22:** 946-957, 1997.

CRICUN R, CRICUN ME: *Imaging Modalities of Spinal Disorders*. WB Saunders, Philadelphia, 1988.

CROCK HV, YOSHIZAWA H: The blood supply of the lumbar vertebral column. *Clin Orthop* **115:** 6-21, 1976.

DE PALMA AF, ROTHMAN H: *The Intervertebral Disc*. WB Saunders, Philadelphia, 1970.

DELAMARTER RB, BOHLMAN HH, BODNER D, BIRO C: Neurologic function after experimental cauda equina compression. Cystometrograms versus cortical-evoked potentials. *Spine* **15:** 864-870, 1990.

DUBNER R, RUDA MA: Activity-dependent neuronal plasticity following tissue injury and inflammation. *Trends Neurosci* **15:** 96-103, 1992.

GATHIER JC: Radicular disorders due to lumbar discopathy (Hernia nuclei pulposi). In: *Handbook of Clinical Neurology*. Vol. 20, PJ VINKEN, GW BRUYN (eds), Elsevier, New York, 1976, pp 573-604.

GILBERT RW, KIM JH, POSNER JB: Epidural spinal cord compression from metastatic tumor: diagnosis and treatment. *Ann Neurol* **3:** 40-51, 1978.

GLEAVE JRW, MACFARLANE R: Prognosis for recovery of bladder function following lumbar central disc prolapse. *Br J Neurosurg* **4:** 205-210, 1990.

GRZYBICKI D, GEBHART GF, MURPHY S: Expression of nitric oxide synthase type II in the spinal cord under conditions producing thermal hyperalgesia. *J Chem Neuroanat* **10:** 221-229, 1996.

HALDEMAN S, RUBINSTEIN SM: Cauda equina syndrome in patients undergoing manipulation of the lumbar spine. *Spine* **17:** 1469-1473, 1992.

HERBISON AE, SIMONIAN SX, NORRIS PJ, EMSON PC: Relationship of neuronal nitric oxide immunoreactivity to GnRH neurons in the ovariectomized and intact female rat. *J Neuroendocrinol* **8:** 73-82, 1996.

HITCHINS RN, BELL DR, WOODS RL, LEVI JA: A prospective randomized trial of single-agent versus combination chemotherapy in meningeal carcinomatosis. *J Clin Oncol* **5:** 1655-1662, 1987.

HUMPHREY PRD: Degenerative and inflammatory diseases of the spine: neurological consequences. *Curr Opin Neurol Neurosurg* **3:** 576-580, 1990.

IWAMOTO H, KUWAHARA H, MATSUDA H, NORIAGE A, YAMANO Y: Production of chronic compression of the cauda equina in rats for use in studies of lumbar spinal canal stenosis. *Spine* **20:** 2750-2757, 1995.

JARADEH S: Cauda equina syndrome: a neurologist's perspective. *Region Anesth* **8:** 473-480, 1993.

KAWAKAMI M, TAMAKI T: Morphologic and quantitative changes in neurotransmitters in the lumbar spinal cord after acute or chronic mechanical compression of the cauda equina. *Spine* **17:** 13-17, 1992.

KIM SH, CHUNG JM: An experimental model for peripheral neuropathy produced by segmental spinal nerve ligation in the rat. *Pain* **50:** 355-363, 1992.

KITTO KF, HALEY JE, WILCOX GL: Involvement of nitric oxide in spinally mediated hyperalgesia in the mouse. *Neurosci Lett* **148:** 1-5, 1992.

KONNO S, OLMARKER K, BYRÖD G, RYDEVIK B, KIKUCHI S: Intermittent cauda equina compression. An experimental study of the porcine cauda equina with analyses of nerve impulse conduction properties. *Spine* **20:** 1223-1226, 1995a.

KONNO S, YABUKI S, SATO K, OLMARKER K, KIKUCHI S: A model for acute, chronic and delayed graded compression of the dog cauda equina. Presentation of the gross, microscopic and vascular anatomy of the dog cauda equina and accuracy in pressure transmission of the compression model. *Spine* **20:** 2758-2764, 1995b.

KUO DC, HISAMITSU T, DE GROAT WC: A sympathetic projection from sacral paravertebral ganglia to the pelvic nerve and to postganglionic nerves on the surface of the urinary bladder and large intestine of the cat. *J Comp Neurol* **226:** 76-86, 1984.

KURU M: Nervous control of micturition. *Physiol Rev* **45:** 425-494, 1965.

MAO GP, KONNO S, ARAI I, OLMARKER K, KUKUCHI S: Chronic double-level cauda equina compression. An experimental study on the dog cauda equina with analyses of nerve conduction velocity. *Spine* **23:**1641-1644, 1998.

MARŠALA J, ŠULLA I, JALČ P, ORENDÁČOVÁ J.: Multiple protracted cauda equina constrictions cause deep derangement in the lumbosacral spinal cord circuitry in the dog. *Neurosci Lett* **193:** 97-100, 1995.

MARTIN WD, FLETCHER T, BRADLEY W: Innervation of feline perineal musculature. *Anat Rec* **180:** 15-30, 1974.

MATSUSHITA M, IKEDA M, HOSOYA Y: The location of spinal neurons with long descending axons (long descending propriospinal tract neurons) in the cat: a study with the horseradish peroxidase technique. *J Comp Neurol* **184:** 63-80, 1979.

MELLER ST, GEBHART GF: NO and nociceptive processing in the spinal cord. *Pain* **52:** 127-136, 1993.

MELLER ST, DYKSTRA C, GEBHART GF: Production of endogenous nitric oxide and activation of soluble guanylate cyclase are required for N-methyl-D-aspartate-produced facilitation of the nociceptive tail-flick reflex. *Eur J Pharmacol* **214:** 93-96, 1992.

MORGAN C, NADELHAFT I, DE GROAT WC: The distribution of visceral primary afferents from the pelvic nerve to Lissauer's tract and the spinal gray matter and its relationship to the sacral parasympathetic nucleus. *J Comp Neurol* **201:** 415-440, 1981.

OLMARKER K: Spinal nerve root compression. Acute compression of the cauda equina studied in pigs. *Acta Orthop Scand* Suppl 62**:** 242, 1991.

OLMARKER K, RYDEVIK B: Single versus double level nerve root compression: an experimental study on the porcine cauda equina with analyses of nerve impulse conduction properties. *Clin Orthop* **279:** 35-39, 1992.

OLMARKER K, RYDEVIK B, HOLM S: Edema formation in spinal nerve roots induced by experimental, graded compression. An experimental study on the pig cauda equina with special reference to differences in effects between rapid and slow onset of compression. *Spi*ne **14:** 569-573, 1989a.

OLMARKER K, RYDEVIK B, HOLM S, BAGGE U: Effects of experimental graded compression on blood flow in spinal nerve roots. A vital microscopic study on the porcine cauda equina. *J Orthop Res* **7:** 817-823, 1989b.

OLMARKER K, HOLM S, RYDEVIK B: Importance of compression onset rate for the degree of impairment of impulse propagation in experimental compression injury of the porcine cauda equina. *Spine* **15:** 416-419, 1990a.

OLMARKER K, HOLM S, RYDEVIK B: More pronounced effects of double level compression than single level compression on impulse propagation in the porcine cauda equina. *Proceedings of the International Society for the Study of the Lumbar Spine.* Boston, June, 1990b.

OLMARKER K, RYDEVIK B, HANSSON T, HOLM S: Compression-induced changes of the nutritional supply to the porcine cauda equina. *J Spinal Disord* **3:** 25-29, 1990c.

OLMARKER K, HOLM S, ROSENQVIST AL, RYDEVIK B: Experimental nerve root compression. Presentation of a model for acute, graded compression injury of the porcine cauda equina, with analyses of the normal nerve and vascular anatomy. *Spine* **16:** 61-69, 1991.

OLMARKER K, TAKAHASHI K, RYDEVIK B: Anatomy and compression-pathophysiology of the nerve roots of the lumbar spine. In: *Spinal Stenosis,* GBJ ANDERSON, T MACNEILL (eds), Mosby Year Book, St. Louis, 1992, pp 77-90.

OLMARKER K, RYDEVIK B, NORDBORG C: Autologous nucleus pulposus induces neurophysiologic and histologic changes in porcine cauda equina nerve roots. *Spine* **18:** 1425-1432, 1993.

ORENDÁČOVÁ J, ČÍŽKOVÁ D, KAFKA J, LUKÁČOVÁ N, MARŠALA M, ŠULLA I, MARŠALA J, KATSUBE N: Cauda equina syndrome. *Prog Neurobiol* **64:** 613-37, 2001.

ORENDÁČOVÁ J, MARŠALA M, ŠULLA I, KAFKA J, JALČ P, ČÍŽKOVÁ D, TAIRA Y, MARŠALA J: Incipient cauda equina syndrome as a model of somatovisceral pain in dogs: spinal cord structures involved as revealed by the expression of c-fos and NADPH diaphorase activity. *Neuroscience* **95:** 543-557, 2000.

OSSIPOV MH, BIAN D, MALAN TP, LAI J, PORRECA F: Lack of involvement of capsaicin-sensitive primary afferents in nerve-ligation injury induced tactile allodynia in rats. *Pain* **79:** 127-133, 1999.

PEDOWITZ RA, RYDEVIK BL, SWENSON MR, HARGENS AR, MASSIE JB, MYERS RR, GARFIN SR: Differential recovery of motor and sensory nerve root conduction following 2 or 4 hours of graded compression of the pig cauda equina. *Proceedings of the International Society for the Study of the Lumbar Spine*. Kyoto, May 17, 1989.

PULLEN AH, HUMPHREYS P: Protracted elevation of neuronal nitric oxide synthase immunoreactivity in axotomised adult pudendal motor neurons. *J Anat* **81:** 307-316, 1999.

RYDEVIK B: Neurophysiology of cauda equina compression. *Acta Orthop Scand* Suppl 251**:** 52-55, 1993.

SATO K, KONNO S, YABUKI S, MAO GP, OLMARKER K, KIKUCHI S: A model for acute, chronic, and delayed graded compression of the dog cauda equina: neurophysiologic and histologic changes induced by acute, graded compression. *Spine* **22:** 2386-2391, 1995.

SAYEGH FE, KAPETANOS GA, SYMEONIDES PP, ANOGIANNAKIS G, MADENTZIDIS M: Functional outcome after experimental cauda equina compression. *J Bone Joint Surg* **79:** 670-674, 1997.

SHI TJ, HOLMBERG K, XU ZQ, STEINBUSCH H, DE VENTE J, HÖKFELT T: Effect of peripheral nerve injury on cGMP and nitric oxide synthase levels in rat dorsal root ganglia: time course and coexistence. *Pain* **78:** 171-180, 1998.

SORENSEN SC, EAGAN RT, SCOTT M: Meningeal carcinomatosis in patients with primary breast or lung cancer. *Mayo Clin Proc* **59:** 91-94, 1984.

STEEL JH, TERENGHI G, CHUNG JM, NA HS, CARLTON SM, POLAK JM: Increased nitric oxide synthase immunoreactivity in rat dorsal root ganglia in a neuropathic pain model. *Neurosci Lett* **169:** 81-84, 1994.

STROSZNAJDER J, CHALIMONIUK M: Biphasic enhancement of nitric oxide synthase activity and cGMP level following brain ischemia in gerbils. *Acta Neurobiol Exp (Warsz)* **56:** 71-81, 1996.

THOR KB, MORGAN C, NADELHAFT I, HOUSTON M, DE GROAT WC: Organization of afferent and efferent pathways in the pudendal nerve of the female cat. *J Comp Neurol* **288:** 263-279, 1989.

TSUKADA Y, FOUAD A, PICKREN JW, LANE WW: Central nervous system metastasis from breast carcinoma: autopsy study. *Cancer* **52:** 2349-2354, 1983.

VIZZARD MA, ERDMAN SL, ERICKSON VL, STEWART RJ, ROPPOLO JR, DE GROAT WC: Localization of NADPH diaphorase in the lumbosacral spinal cord and dorsal root ganglia of the cat. *J Comp Neurol* **339:** 62-75, 1994.

VIZZARD MA, ERICKSON K, DE GROAT WC: Localization of NADPH diaphorase in the thoracolumbar and sacrococcygeal spinal cord of the dog. *J Auton Nerv System* **64:** 128-142, 1997.

WIESEL SW, TSOURMAS N, FEFFER HL, CITRIN CM, PATRONAS N: A study of computer-assisted tomography. 1. The incidence of positive CAT scans in an asymptomatic group of patients. *Spine* **9:** 549-551, 1984.

WOOLF CJ: Evidence for a central component of postinjury pain hypersensitivity. *Nature* **306:** 686-688, 1983.

YAMAGUCHI K, MURAKAMI M, TAKAHASHI K, MORIYA H, TATSUOKA H, CHIBA T: Behavioral and morphologic studies of the chronically compressed cauda equina. Experimental model of lumbar spinal stenosis in the rat. *Spine* **24:** 845-851, 1999.

YAP HY, YAP BS, TASHIMA CK, DI STEFANO A, BLUMENSCHEIN GR: Meningeal carcinomatosis in breast cancer. *Cancer* **42:** 283-286, 1978.

YEZIERSKI RP, LIU S, RUENES GL, BUSTO R, DIETRICH WD: Neuronal damage following intraspinal injection of a nitric oxide synthase inhibitor in the rat. *J Cereb Blood Flow Metab* **16:** 996-1004, 1996.

ZHANG X, VERGE V, WIESENFELD-HALLIN Z, JU G, BREDT D, SNYDER SH, HÖKFELT T: Nitric oxide synthase-like immunoreactivity in lumbar dorsal root ganglia and spinal cord of rat and monkey and effect of peripheral axotomy. *J Comp Neurol* **335:** 563-575, 1993.

Reprint requests

Prof. Jozef Maršala, M.D.. Institute of Neurobiology, Slovak Academy of Sciences, Šoltésovej 4, 040 01 Košice, Slovak Republic. E-mail: marsala@saske.sk